

Comparison between PEMFC Water Management Model and in-situ Water Transfer Measurements

Pierre Sauriol¹, Gwang-Soo Kim², H. Tony Bi¹, Jürgen Stumper² and Jean St-Pierre²

(1) Department of Chemical and Biological Engineering, UBC, Vancouver, BC, Canada

(2) Ballard Power Systems, Burnaby, BC, Canada

ABSTRACT

This work describes the design steps and demonstrates the capabilities of a novel water transfer factor measurement apparatus for the purpose of experimental analysis, water management model validation and tailoring. Several measurement concepts were screened on the basis of their water transfer factor accuracy using a Monte-Carlo approach. The most promising concept was assembled and tested to assess its actual measurement accuracy. Combining cathode and anode measurements, the simulated water transfer factor accuracy was typically better than ± 0.01 . The measurement strategy was finally implemented on a real PEMFC and several series of tests were conducted. Experimental data was in good agreement with a recently proposed model under moderately high pressure (200 kPa) and current densities (above 0.3 A/cm^2), but indicates that the model tends to underestimate the back diffusion of the water from the cathode to the anode especially at low current densities.

INTRODUCTION

Water management has become one of the crucial aspects in the design and operation of PEMFCs on way to their wide spread commercialization. The challenges of water management have been addressed in many ways: membrane-electrode assembly (MEA) designs, flow field designs, refined strategy for PEMFC operation, experimental evaluation and fundamental modeling. Although fundamental modeling has the added advantage of incorporating and discriminating between several aspects of the PEMFC operation, the results from modeling efforts are only as good as their inputs. Conflicting data and/or predictions of the water transfer factor in PEMFC reported in the literature has motivated the experimental effort described herein.

Modelers first introduced the water transfer factor to simplify the writing of the mass balance equations. The water transfer factor is defined as the net water flux across the membrane divided by the water production flux and is positive for water going from the anode to the cathode. It incorporates water transferred by electro-osmotic drag, diffusion and convection. The water transfer factor is found to be a determining aspect in the membrane's hydration state, hence its conductivity. From an experimental standpoint, the water transfer factor has seldom been reported in the literature. This can be explained by the difficulty in achieving water balance measurements that are accurate enough to allow for an accurate determination of the water flux across the membrane. The water balance measurements are further made difficult by the likely two-phase nature of the flows exiting the PEMFCs. Janssen and Overvelde (1) and Voss et al. (2), have generated data that allows for the calculation of the overall water transfer factor in PEMFC stacks by water collection on the PEMFC stack outlet streams. Mench et al. (3) reported in-situ water concentration measurements. They used a gas chromatograph to measure amongst others the water content of the gas-phase. Despite these limitations in measuring the water transfer factor on running PEMFCs, several efforts focusing on the individual contributing mechanisms have been achieved in the past two

decades. It's chiefly through the results from such efforts that modelers (4-6) were able to predict the water transfer factor for PEMFCs.

It is generally accepted that three mechanisms are responsible for the water transfer across the MEA: electro-osmotic drag, diffusion and convection. Most of the efforts on these mechanisms targeted the determination of the electro-osmotic drag contribution. This mechanism has often been considered the leading contributor to the water transfer factor. Several approaches have been used to determine this parameter. Some are limited to membranes kept under saturated conditions (7-8). Okada et al. (9) summarize some of their work conducted using the streaming potential technique. Recent experimental work achieved on sub-saturated membranes showed that the results from saturated membranes could not be directly extrapolated to sub-saturated conditions (10-11). They found that the electro-osmotic drag coefficient remained fairly constant with varying membrane hydration under sub-saturated conditions. In the latter, the authors report a drag coefficient of one water molecule per proton in the sub-saturated conditions for several poly-perfluorosulfonic acid membranes. PEMFC simulations using this reduced electro-osmotic drag were implemented by few authors since then and proved to be of great importance on the water transfer factor. Berg et al. (12) and Hsing and Futerko (13), were amongst the first to predict negative water transfer factors, indicating that the back diffusion from the cathode to the anode can, under certain conditions, be the dominating form of transfer. Recently, Karimi and Li (14) have adopted a theoretical approach to investigate the parameters most influential on the electro-osmotic drag. Their approach considers liquid water in the membrane pores and is probably limited to saturated conditions.

Water diffusion has also been the target of experimental efforts. These have focused on the membrane diffusion alone, not as part of an MEA. Zawodzinski et al. (15) have evaluated the water diffusion rate in Nafion membranes using an NMR technique. Nguyen and Vanderborgh (16) have investigated the water diffusion rate within a membrane with low water content by thermo gravimetric analysis. Okada et al. (9) derived a diffusion coefficient from the streaming potential approach with the assumption of a linear relationship between the electro-osmotic drag and the water content. Although limited, these efforts indicated a temperature dependency. Often neglected in models, the purely convective transport of water through the membranes has been the subject of very few efforts. Okada et al. (9,17) have looked into these aspects under saturated conditions using the streaming potential technique.

The basis for this work is the model proposed by Berg et al. (12). In their effort, the authors built a 1+1D model able to predict the cell voltage, the current density, the water transfer factor and the membrane water content along the length of a PEMFC channel. Key model parameters were optimized by comparing in-situ current distributions from a running PEMFC as described by Stumper et al. (18). As a result, the model predictions are in good agreement with the experimental current density profiles obtained over a wide range of operating conditions. The model predicts water transfer factors that are generally lower to those predicted by other models (e.g. Springer et al. (4)). As very few experimental data on the overall water transfer factor in PEMFCs and even less on its distribution have been achieved thus far, it is desired to develop a measurement apparatus that will allow for the experimental determination of the water transfer factor on a running 300 cm² PEMFC. These measurements will be used for the purpose of model validation and tailoring.

DEFINITIONS AND CALCULATIONS

This section contains definitions that are required to fully understand the calculation effort deployed in the measurement concept development and evaluation.

Definitions

The water transfer factor is one of the parameters used in most models derived from that of Springer et al. (4). This factor combines the water fluxes across the membrane from three mechanisms: the electro-osmotic drag, the diffusive transfer and the convective transfer (often neglected in models). The water transfer factor used throughout this work is defined locally and expressed by equation 1.

$$\alpha \equiv \frac{Q_{H_2O, a \rightarrow c}}{Q_{H_2O, rx}} \quad (1)$$

Since it is desired to reproduce the water transfer factor distribution profile along a 300 cm² PEMFC and that the measurement of the water transfer factor is likely to be achieved by mass balance, the generation of the profile will be achieved by dividing the 300 cm² PEMFC into consecutive sub-cells. The sub-cells are run one at a time, conceptually feeding one into the other. The outlet conditions will be measured and the inlet conditions of the subsequent sub-cell recreated. This strategy will allow for the measurement of the water transfer factor profile that will be compared with the model-based distributions. The relationships that exist between the local and average water transfer factor need to be considered for comparison purposes. The average water transfer factor can be determined from the local water transfer factor and current density distributions according to equation 2. The average water transfer factors are obtained from equations 3a and 3b for the cathode and anode respectively.

$$\bar{\alpha} = \frac{\int \alpha j dA}{\int j dA} \quad (2)$$

$$\bar{\alpha}_c = \frac{n_{H_2O, c, out} - n_{H_2O, c, in}}{n_{H_2O, rx}} - 1 \quad (3a)$$

$$\bar{\alpha}_a = \frac{n_{H_2O, a, in} - n_{H_2O, a, out}}{n_{H_2O, rx}} \quad (3b)$$

Measurement Concept Development

Several measurement concepts were considered as potential candidates for the water transfer measurement apparatus. Some of these concepts relied on mass, volumetric flow, dew point and concentration measurements. Ultimately, the down-selection of the measurement concept was achieved on the basis of the expected water transfer factor

Table I - Range of Key Operating Parameters

Operating parameter	Sub-cell size (cm ²)		
	300	50	18.75
Current density (A/cm ²)	0.017-1.00	0.015-1.08	0.015-1.08
Cathode flow rate (mol/s)	3.1x10 ⁻⁴ -6.7x10 ⁻³	3.0x10 ⁻⁴ -6.7x10 ⁻³	2.9x10 ⁻⁴ -6.7x10 ⁻³
Cathode O ₂ molar fraction (dry)	0.21	0.11-0.21	0.10-0.21
Anode flow rate (mol/s)	1.3x10 ⁻⁴ -2.5x10 ⁻³	1.1x10 ⁻⁴ -2.5x10 ⁻³	1.0x10 ⁻⁴ -2.5x10 ⁻³
Cathode water rate (mol/s)	5.8x10 ⁻⁵ -6.8x10 ⁻⁴	5.8x10 ⁻⁵ -2.2x10 ⁻³	5.8x10 ⁻⁵ -2.3x10 ⁻³
Anode water rate (mol/s)	1.7x10 ⁻⁵ -1.9x10 ⁻⁴	1.6x10 ⁻⁵ -2.8x10 ⁻⁴	1.6x10 ⁻⁵ -2.8x10 ⁻⁴
Produced water (mol/s)	2.6x10 ⁻⁵ -1.6x10 ⁻³	4.1x10 ⁻⁶ -2.8x10 ⁻⁴	1.5x10 ⁻⁶ -1.1x10 ⁻⁴
Transferred water (mol/s)	1.6x10 ⁻⁶ -1.1x10 ⁻⁴	-8.2x10 ⁻⁵ -4.5x10 ⁻⁵	-7.0x10 ⁻⁵ -1.7x10 ⁻⁵
Water transfer factor	0.0391-0.0973	-0.366-0.186	-1.08-0.190

accuracy. For this, Monte Carlo generated virtual experiments of the most promising concepts were conducted using the specified accuracy and sensitivity of the key components for the considered measurement concept. This section summarizes the down-selection effort and presents three of the considered configurations.

In order to develop a measurement/calculation concept for the water transfer factor measurement apparatus, a certain number of parameters were specified. The water transfer factor is desired with ± 0.03 accuracy. This accuracy should cover a wide range of operating conditions with current densities ranging from 0.02 to 1 A/cm² for a 300 cm² PEMFC. The instrument should offer continuous data collection with the capability of analyzing the performance of the PEMFC to step changes in humidification and current density.

For the measurement concept development, the expected water transfer factor and current density profiles, necessary to estimate the conditions along the PEMFC channels were obtained using the model developed by Berg et al. (12). This choice was arbitrary, however it is believed that the accurate measurement of small water transfer factors such as the ones predicted by Berg et al. will be more difficult than the larger ones predicted by other models. The range of key operating parameters and the corresponding model-based current densities, water transfer rates and water transfer factors are determined and presented in Table I for 3 considered sub-cell sizes (300, 50 and 18.75 cm²). Those key operating parameters provided the basis for the down-selection of the instruments required for the water transfer factor measurement apparatus.

Several sensitivity analyses were achieved to determine the most important quantities that influence the accuracy of the water transfer factor measurement. It was found that accurate measurements and control of the water addition rate could be achieved by injecting water from syringe pumps. This will enable reproducible water addition rates, the ability to generate rapid changes in humidification as well as over saturated stream conditions. On the outlet side, accurate concentration measurement by the use of infrared sensors was selected as the most promising way to achieve online measurements. Infrared sensors for water measurements are available in various sizes, accuracy and sensitivity ratings, time resolutions, communication interfaces and prices. For a single diagnostic apparatus, the Licor LI-7000 was deemed to possess good accuracy, excellent sensitivity and time resolution, and convenient communication formats at a reasonable cost. Figure 1 depicts three measurement concepts for which virtual experiments were generated. As the water transfer factor measurement can

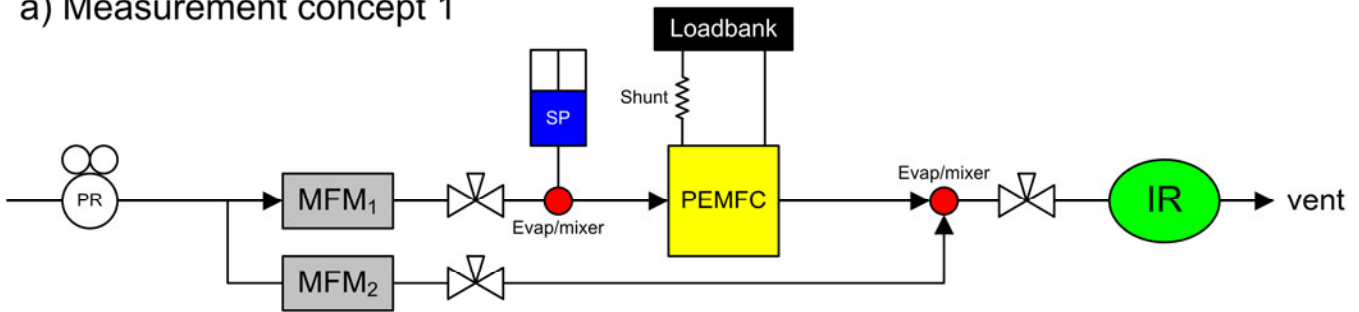
be achieved on both anode and cathode independently, the measurement concepts are only illustrated for one. In a), dry gas enters the system and goes through a pressure regulator (PR) where the outlet pressure is kept at a pressure corresponding to the mass flow meters (MFM) calibration pressure. Given the range of operation, several mass flow meters are required to avoid their use at low flow rate (relative to their full scale capability) where greater relative errors are expected. Prior to entering the PEMFC, the dry stream goes through an evaporative mixer where the stream is humidified to the desired level by direct injection of water from a syringe pump (SP). The use of a syringe pump makes it possible to achieve two-phase conditions required by some of the test conditions. The net load is measured by voltage measurement across a calibrated shunt. The PEMFC outlet, which may present itself as a two-phase stream, is blended with a dry gas stream and heated in order to respect the operation limits of the infrared sensor (IR) and prevent liquid water accumulation in the lines between the PEMFC and the infrared sensor. Before entering the infrared sensor, the mixture goes through a backpressure valve to allow for the adjustment of the PEMFC pressure. The gas entering the infrared sensor is vented to a low-pressure line. For this configuration, the water transfer factor for the cathode side can be expressed as in equation 4 (the anode side can be determined according to 3b). In b), the mass flow meters are taken out of the water transfer factor calculation and replaced by a preliminary water injection (SP_{pre}) and water concentration measurement (IR_{pre}). The total flow rate required in the water transfer factor calculation is determined from the concentration and water injection rates. A flow-metering device is required to adjust the PEMFC inlet stream, but is not involved in the calculation. Its accuracy will not affect the water transfer calculations. The water transfer calculation for this configuration is given by equation 5. In c), a reference water injection (SP_{ref}) step is introduced in order to allow for the water concentration and flow rate measurement to be expressed as a function of the water injection rates (i.e. a one point calibration). Equation 6 gives the expression of the water transfer factor calculation for this configuration.

$$\bar{\alpha}_c = \frac{\left(\frac{x_{H_2O,c,out}}{1-x_{H_2O,c,out}} \right) \left(n_{MFM1,c} + n_{MFM2,c} + \frac{v_{O_2}}{v_{e^-}} \frac{I}{F} \right) - n_{H_2O,c,in}}{\frac{v_{H_2O}}{v_{e^-}} \frac{I}{F}} - 1 \quad (4)$$

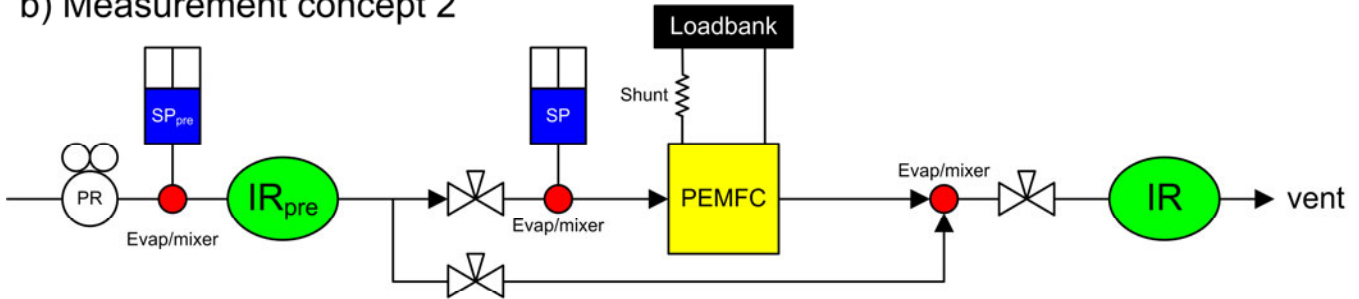
$$\bar{\alpha}_c = \frac{\left(\frac{x_{H_2O,c,out}}{1-x_{H_2O,c,out}} \right) \left[n_{H_2O,c,pre} \left(\frac{x_{H_2O,c,pre}}{1-x_{H_2O,c,pre}} \right) + \frac{v_{O_2}}{v_{e^-}} \frac{I}{F} \right] - n_{H_2O,c,pre} - n_{H_2O,c,in}}{\frac{v_{H_2O}}{v_{e^-}} \frac{I}{F}} - 1 \quad (5)$$

$$\bar{\alpha}_c = \frac{n_{H_2O,c,ref} \left(\frac{x_{H_2O,c,out}}{1-x_{H_2O,c,out}} \right) \left(\frac{1-x_{H_2O,c,ref}}{x_{H_2O,c,ref}} \right) \left(\frac{n_{MFM1,c} + n_{MFM2,c} + \frac{v_{O_2}}{v_{e^-}} \frac{I}{F}}{n_{MFM1,c,ref} + n_{MFM2,c,ref}} \right) - n_{H_2O,c,in}}{\frac{v_{H_2O}}{v_{e^-}} \frac{I}{F}} - 1 \quad (6)$$

a) Measurement concept 1



b) Measurement concept 2



c) Measurement concept 3

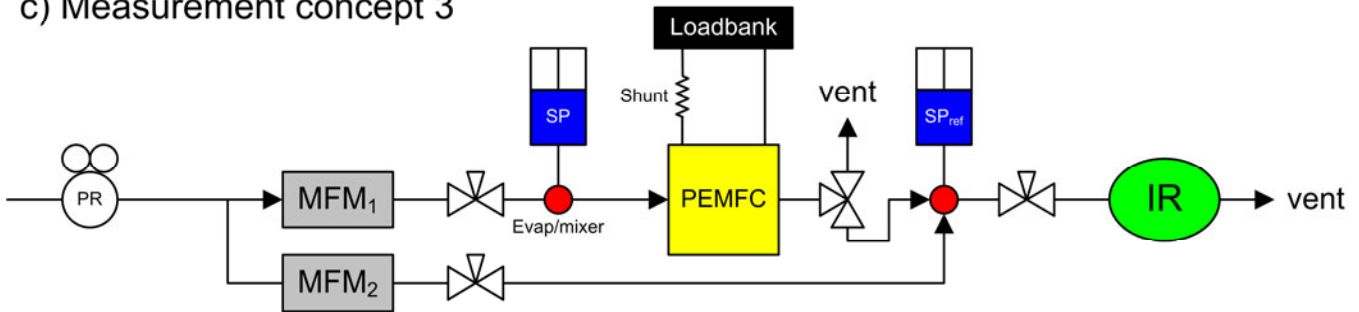


Figure 1 – Three Measurements Concepts Utilizing Syringe Pump and Infrared Sensor

The Monte Carlo virtual experiments covering the full range of operating conditions were generated on the basis of the instrument specifications and a number of operational considerations, which are summarized in Tables II and III respectively. The Monte Carlo analysis is conducted as an evaluation tool in order to rank different measurement concepts, to identify the accuracy determining components and to determine scaling rules. For these calculations, the assumption of steady state is made to simplify the analysis. For each condition tested, 100000 randomly generated calculations were achieved. The results of the Monte Carlo virtual experiments are presented in Figure 2 for both cathode and anode based measurements. In a) and b), the average computed water transfer factors are compared with the model-based values which served to define the conditions. In a) instruments are considered exact. The absence of significant error confirms that all three approaches can potentially lead to the determination of the water transfer factor. In b) the instruments performance is described using the specifications from Table II. The results show that measurement concept 2 is biased and would result in greater water transfer factors when measuring on the cathode side and towards lower water transfer factors when measuring on the anode side. In c), the standard deviation of the computed water transfer factors is plotted against the water ratio, defined in equation 7.

Table II - Instruments Specifications

Measurement	Manufacturer: model	Accuracy ¹	Sensitivity
Gas flow	Hastings Instruments: 200 series	±1% full scale (linearity)	±0.1% full scale
Water injection rate	KDScientific: KDS210	<±1% (manufacturer) <±0.1% (experiment)	±0.1%
Shunt resistance	unknown	±0.001mΩ	NA
Voltage	HP/Agilent: HP34970A	±0.004% of reading + 7μV (3σ)	±90 dB
Water molar fraction	Licor: LI-7000 CO ₂ /H ₂ O analyzer	±1% (linearity)	±2.24 ppm @ 0 ±4.47 ppm @ 0.01

(1) When not specified, accuracy considered to be defined on a 1σ basis

$$Water\ ratio = \frac{n_{H_2O,out}}{\frac{v_{H_2O}}{v_e} I} \quad (7)$$

Four key observations can be deduced from these results: 1) Under most operating conditions, the anode side measurements yield more accurate water transfer factors; 2) Unless grossly oversized mass flow meters are to be used, the dual infrared sensor strategy yields the worst accuracies of the three concepts considered; 3) The accuracy of the water transfer factor measurement is primarily dictated by the infrared sensor accuracy and to a lesser degree by the mass flow meter accuracies; 4) The generation of a reference injection, improves the accuracy of the measurement by eliminating the subtraction of large numbers from different sources in the calculation of the water transfer factor (refer to equations 4 through 6). Given the results of the Monte Carlo virtual experiments, measurement concept 3 was retained for experimental evaluation of the water transfer factor accuracy.

Table III - Operational Consideration for the Monte Carlo Virtual Experiment Simulation

Variable	Conditions	Measurement concept
Cathode PEMFC stream mass flow meters (MFM ₁)	1, 3 and 9 SLPM	1 and 3
Cathode dilution stream mass flow meters (MFM ₂)	8, 24, 72 and 216 SLPM	1 and 3
Anode PEMFC stream mass flow meters (MFM ₁)	0.4, 1.2 and 3.6 SLPM	1 and 3
Anode dilution stream mass flow meters (MFM ₂)	3, 9 and 27 SLPM	1 and 3
Infrared sensor calibration range	0-0.03 (at accuracy specified in Table II)	1, 2 and 3
Bypass flow rate adjustment	Flow rate set so that water molar fraction at the outlet infrared sensor is less than 0.015 assuming no water transfer	1, 2 and 3
Pre-water injection	Injection rate is 50% of the water rate coming out of the PEMFC assuming no water transfer	2

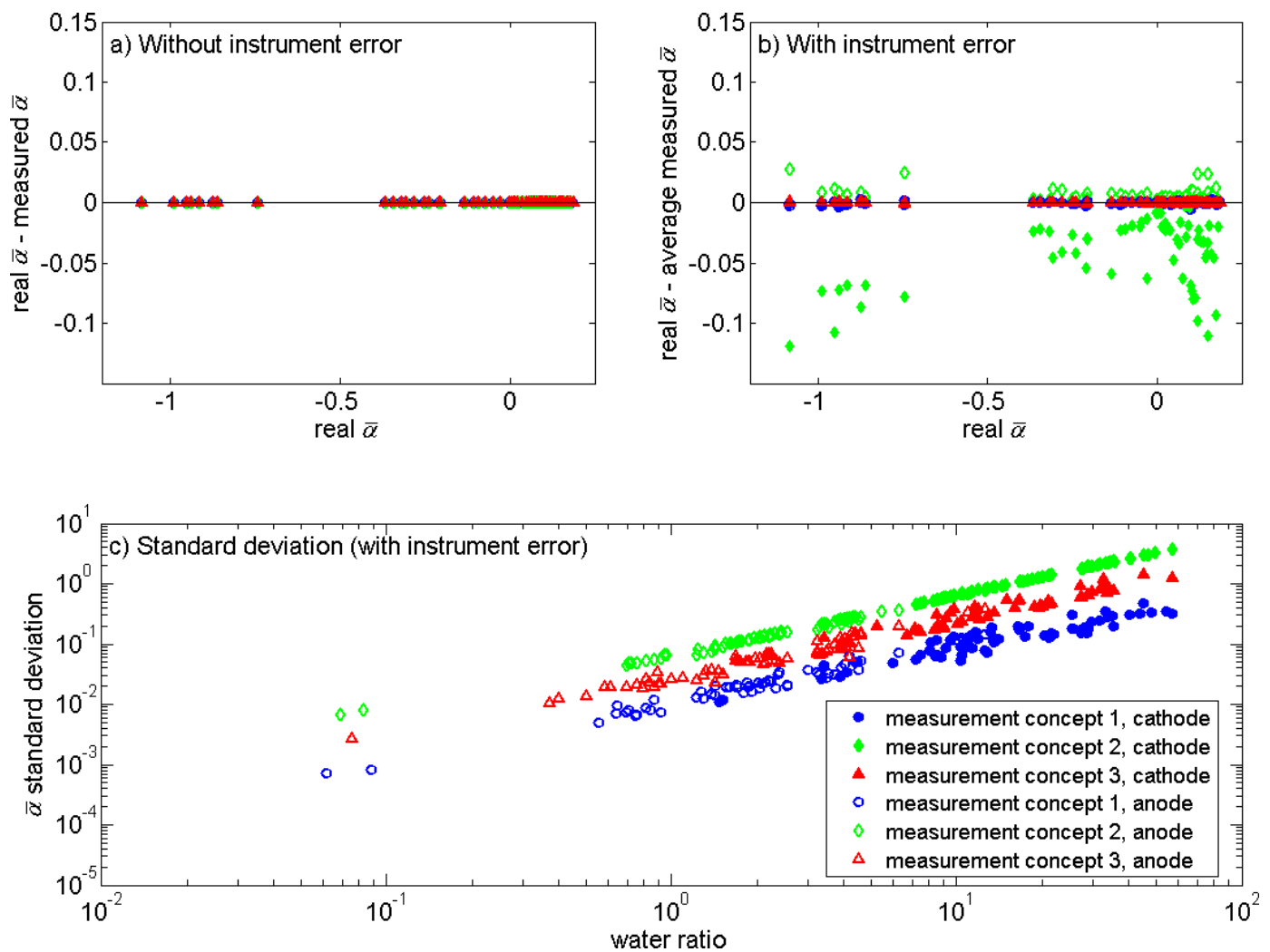


Figure 2 - Results from the Monte Carlo Virtual Experiments: a) difference between the real and measured water transfer factors in the absence of instrument error; b) difference between the real and measured water transfer factors considering instrument error (Monte Carlo virtual experiments); c) standard deviation in the water transfer as a function of the water ratio

EXPERIMENTAL RESULTS AND DISCUSSION

The experimental work is divided into two parts. The first addresses a series of concept validation runs that were performed on a simplified setup to determine the water transfer measurement accuracy. The second is a series of measurements on a running PEMFC.

Concept Validation Experiments

The most promising concept from the Monte Carlo virtual experiments, measurement concept 3, was assembled. In an effort to gather a significant amount of data allowing for the determination of the measurement accuracy, experiments were run using a simplified setup that excluded the PEMFC, an unknown in the water transfer factor determination. Instead, the

PEMFC effect was simulated by varying the water injection rate to levels corresponding to those at the PEMFC outlet under normal operation. Furthermore, these tests provided a good opportunity to gain hands-on understanding of the infrared sensor, the ability to determine the best conditions needed to evaporate varying amounts of water with the dilution gas and the operation of the infrared sensor with hydrogen rich streams.

There are three great differences between the PEMFC operations and the concept validation experiments. 1) In the absence of a reaction, there is no variation in the flow rate due to the gas consumption. 2) The amounts of water produced are not determined from the load measurement. 3) On operating PEMFCs, water slugs are often observed in the outlet stream. The first two points were considered in the Monte Carlo analysis as the simulated fuel cell operation was also considered. The results are reported in Figure 2 and do not show obvious deviation from the normal operation behavior. This indicates that the errors resulting from the load measurement are much less important than the ones associated with the water concentration and the flow rates. As for the third point, its influence on the system operation was simulated by voluntarily favoring a poor mixing at the water injection point during the validation experiments. This was achieved by having low gas velocity at the location where the water was injected (e.g. large tubing), which resulted in the formation of large, low-frequency droplets that mimic the water slugs often observed at the outlet of a PEMFC.

In a first experiment, the response time characteristics of the infrared sensor were investigated. For this, air was used and the water injection rate was varied between 0 and 3×10^{-4} mol/s, for corresponding water ratios ranging between 0 and 1.65. Figure 3 shows the results from this typical concept validation experiment. In a) the raw data from the infrared sensor is presented. On average, the water molar fraction follows the same trends as the injection rate. However, significant fluctuations characterize the water concentration signals. A closer look at the fluctuations (see inserts) reveals that they are very periodic and are the result of large droplets entering the system at the injection point. A simple analysis allows for the estimation of the droplet size (approximately 5.7 mm in diameter) and frequency, which were later qualitatively confirmed by visual observation. The raw data also presents repeated dropouts at an hourly interval. These dropouts result from the use of syringe pumps for the accurate dispensing of the liquid water, which need to be refilled regularly. Even though pairs of syringe pumps are used, the water injection is momentarily altered when swapping from one to the other. For the analysis, those dropouts were left out. Due to the fluctuations in the measured water concentrations, the analysis of the data required some post-treatment, which consisted in the running moving-average filters on the data in order to eliminate the fluctuations associated with the droplets. Once the post-treatment of the water concentration signal is done, the water transfer factor can be readily determined. In b), the expected water transfer factor is plotted along with the experimental values. The results are presented for two different averaging times, 5 and 30 minutes, both of which are in excellent agreement with the expected values. The ideal data-averaging period should be chosen so that the resolution is satisfactory for trends to be observed. On the other hand, the accuracy is related to the difference between the long-term average of the signal and the real value. Here, the simulated water transfer factors are determined with an accuracy better than ± 0.01 , using the average from 90 minutes of operation as the long-term average of the data and the expected values as the real values.

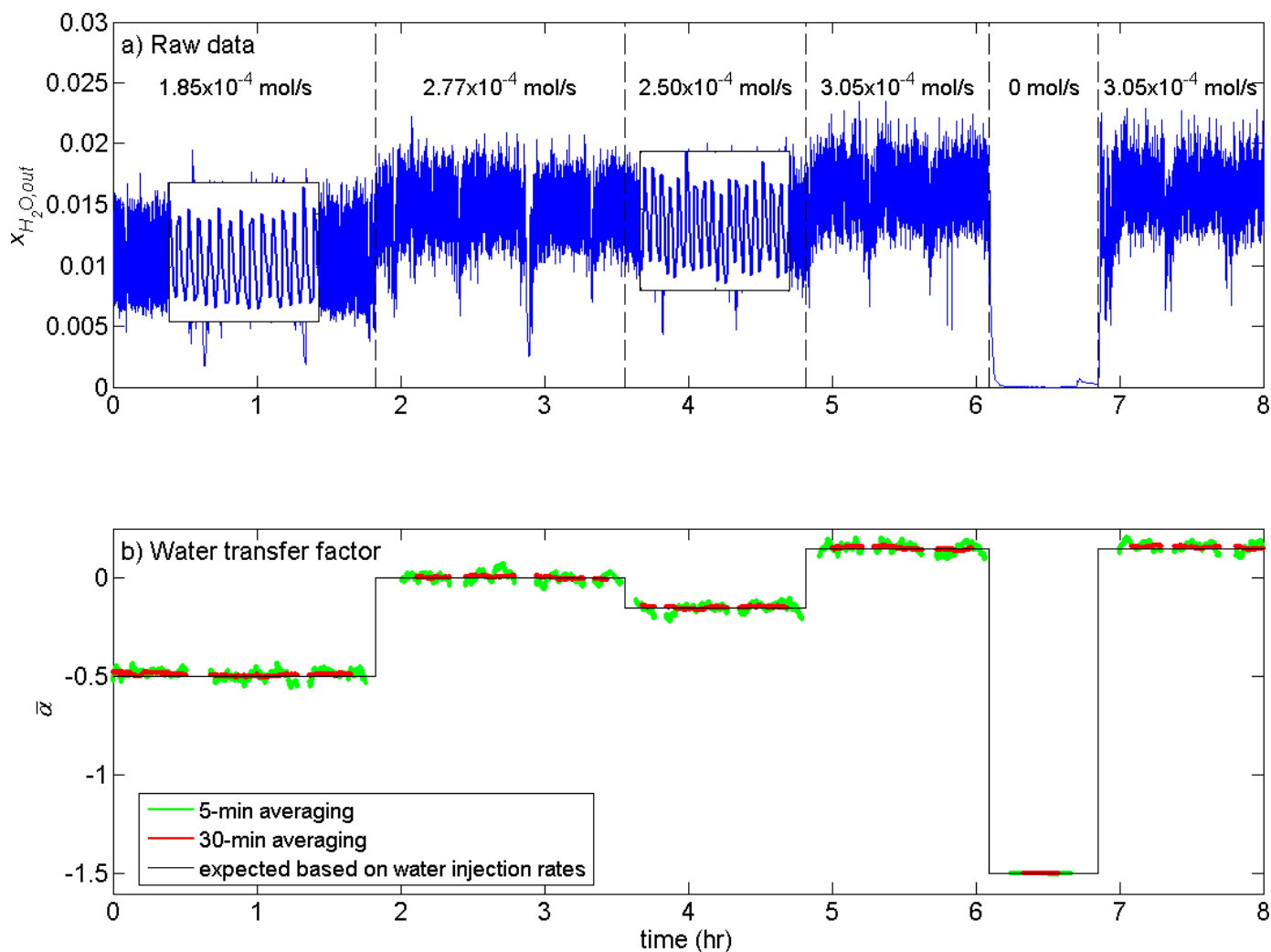


Figure 3 - Typical Raw Data from a Concept Validation Experiment: a) raw data for given injection sequence; b) water transfer factor (water ratio 0 - 1.65)

Several other validation experiments were completed to establish the instrument capability over a broad range of operating conditions. Air, nitrogen, helium and hydrogen were used to determine the effect of the gas composition on the infrared sensor measurement. It is clear from the data that the infrared sensor response with helium and hydrogen differed from the linearity observed with air and nitrogen. This non-linearity of the response with water-hydrogen system could limit the water transfer factor accuracy determined on the anode side. The measurement strategy was adapted to include multiple reference measurements, which will be used to derive a calibration curve. It was found that at least two reference injections were sufficient to generate a calibration that could account for the non-linearity. The results from the concept validation experiments are summarized in Table IV. These experiments show that under the concept validation configuration, the combined cathode and anode measurements allows for the water transfer factor to be determined with an accuracy better than ± 0.01 and confirms that the anode side measurements are more accurate than the cathode side measurements due to the favorable water ratios.

Table IV – Accuracy and Standard Deviation of the Water Transfer Factor Measurements from the Concept Validation Runs Considering 18.75 cm² Sub-cells

Current density ¹	0.267 A/cm ²		1 A/cm ²	
Sub-cell	1	16	1	16
Accuracy				
Cathode	±0.01	±0.25	±0.008	±0.1
Anode	NA	±0.01	NA	±0.01
Standard deviation (instantaneous; 5-minute averaging; 30-minute averaging)				
Cathode	0.2; 0.05; 0.005	0.3; 0.3; 0.06	0.2; 0.02; 0.005	0.5; 0.3; 0.12
Anode	NA	0.8; 0.2; 0.08	NA	0.9; 0.2; 0.06

(1) Based on a 300 cm² PEMFC

PEMFC Measurements

The demonstrated configuration was assembled with a working PEMFC for normal operation. The water transfer factor measurement system was implemented on both cathode and anode for redundancy purposes. The PEMFC used consisted of a 50 cm² sub-cell equipped with a standard MEA with a Nafion 112 membrane and was capable of being operated under the conditions described in Table I.

The first series of tests consisted in determining the water transfer factor profiles along the length of a 300 cm² PEMFC by using the sub-cell approach. For this, the calculations based on the Berg et al. (12) model were achieved for 3 sets of operating conditions described in Table V. The PEMFC calculations were based on a co-current configuration. One run was devoted to each of the sub-cells. The model-predicted current density was averaged for each of the 6 sub-cells and served as input for each sub-cell. The first sub-cell saw the same conditions as the model input. The sub-cell was operated at the same conditions for a 24-hour period. At the end of this period, the net water transfer factor was determined for both cathode and anode. The average water transfer factor was determined by weighting the cathode and anode water transfer factors according to the inverse of their water ratio. The inlet conditions for the following sub-cell were based on the measured outlet. The process was repeated until all the sub-cells were measured. Figure 4 compares the sub-cell measurements to the model-based predictions.

Generally, the water transfer numbers obtained for the cathode and anode are in good agreement with differences typically ranging between 0.02 and 0.05. Again for these runs, the anode side measurements are far more reproducible than the cathode ones. This is especially true in the last three sub-cells where the amount of water in the measured cathode stream is such that the water ratios rapidly increase from 4 to 7, as opposed to a fairly constant 0.65 for

Table V – Operating Conditions for Water Transfer Factor Tests

Test	Current density (A/cm ²)	Cathode			Anode			Coolant	
		Pressure (kPa)	Dewpoint (°C)	Stoic	Pressure (kPa)	Dewpoint (°C)	Stoic	T _{in} (°C)	T _{out} (°C)
1	0.267	210	38	1.8	230	63	1.6	65	69
2	0.133	115	59	1.8	140	53	4.1	60	62
3	0.1	135	60	1.8	155	58	9.6	60	61
4	0.005-1	200	55	>5.4	220	55	>6.0	60	60

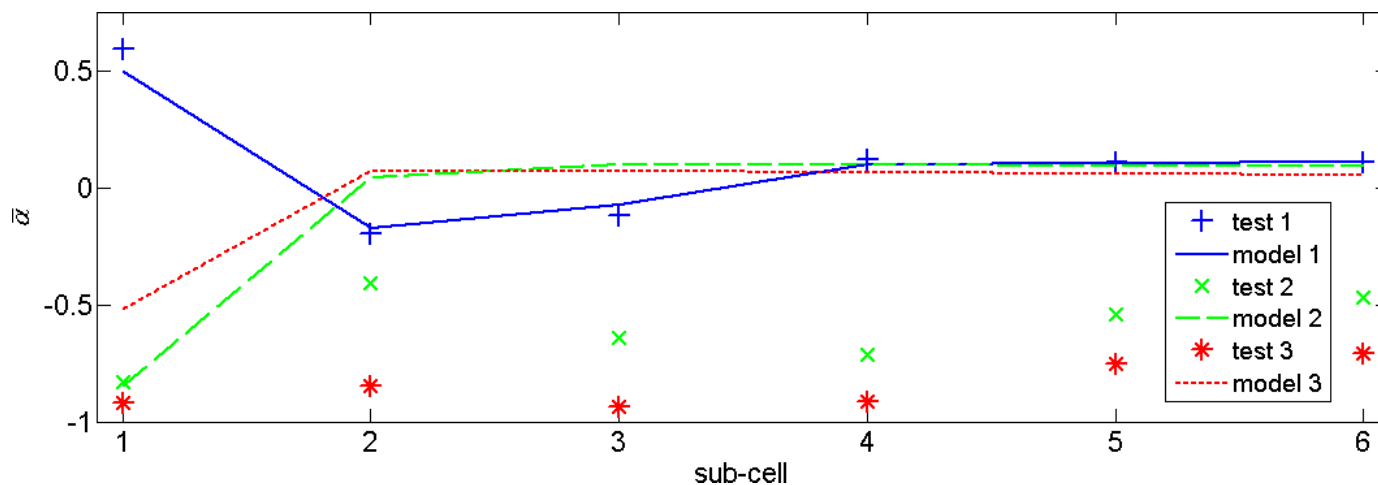


Figure 4 - Experimental and Model-based Water Transfer Factor Profiles

the anode. For test 1, the experimental results and model prediction are in excellent agreement. At the inlet, the relatively dry cathode and humid anode result in a strong water transfer towards the cathode. The quick humidification of the cathode is followed by a sharp decrease in the water transfer. A reversal is observed for the following 2 sub-cells, where the water preferentially transfers from the cathode towards the anode. Probably as a result of the continued hydrogen consumption leading to its saturation, the water transfer factor stabilizes to a value of approximately 0.1 over the last three sub-cells. For these three last sub-cells, the anode side dew point remains relatively constant even though the hydrogen consumption is important. For tests 2 and 3 (low pressure and low current density), the experimental data strongly suggests that the back diffusion of water from the cathode to the anode is a dominant factor even though in most cases the anode side was determined to be saturated. Under the conditions for tests 2 and 3, the operating temperature was found to have a significant influence on the water transfer factor. A variation of 5°C in the coolant temperature was found to result in a 0.3 change in the water transfer factor. On the other hand, the same temperature change was found to have very little influence under the conditions of test 1. The model-based predictions are based on the assumption of a constant voltage. Experimentally, this constant voltage is compromised by the decision to run the sub-cells following the current density profile as predicted by the model. As a result, important voltage discrepancies may exist between the experimental and the model data, especially where the MEA water content is low. As an example, during test 1 these discrepancies were more important at the first sub-cell where the difference was approximately 50 mV. This voltage discrepancy was found to represent a difference of 20% in the current density, if the sub-cell were operated at the model-predicted voltage.

Even though, the generation of water transfer profile can provide great insights on the water management of a PEMFC, the approach is time consuming and often only provides interesting information for the first half of the PEMFC typically until the cathode and anode become saturated (e.g. the last three sub-cells from test 1). In order to systematically analyze the water transfer factor for the purpose of model validation and tailoring, more data needs to be collected covering a wider range of operating conditions (current density, pressure, temperature, composition, RH). This approach was implemented by performing the water transfer factor measurement while generating polarization curves. The results for test 4 are

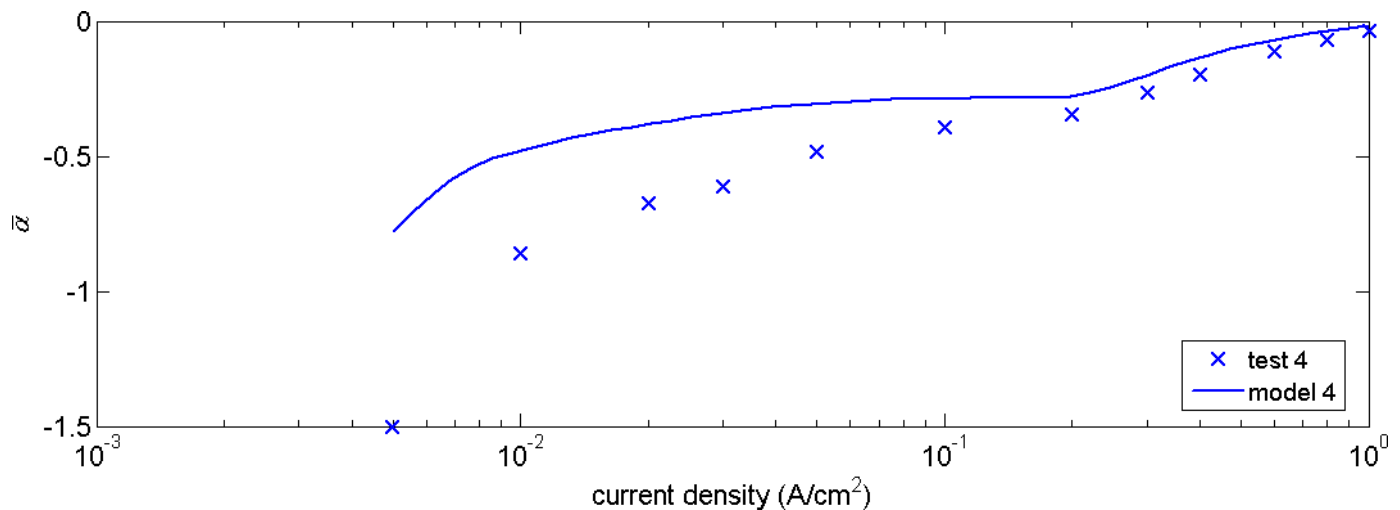


Figure 5 - Experimental and Model-based Water Transfer Factor for Test 4

presented in Figure 5. In this example, the water transfer factor was obtained for 12 current densities in the same time needed to determine the water transfer factor of 3 sub-cells as presented earlier. Generally, the water transfer factor increases as the current density increases. The discrepancies between the experimental water transfer factor and the model-based values diminish as the current density increases. For both, there is a transition zone for current densities around 0.2 A/cm^2 , coinciding with the moment when the streams become saturated with water. By comparison, the discrepancies observed here are comparable to those observed in Figure 4 for tests 2 and 3 under comparable current density and dry conditions. This lends credence to the fact that the lower water transfer factors observed in tests 2 and 3 were the result of the lower current density used in these tests and not the lower pressure.

CONCLUSION

This paper presented the design and initial testing of a novel real-time measurement technique for the accurate measurement of the water transfer factor based on Monte Carlo generated virtual experiments. The measurement concept comprised of infrared sensors for the water concentration measurement and syringe pumps for water injection. Validation experiments showed that combining the cathode and anode measurements, an accuracy of ± 0.01 could be achieved. The measurement apparatus was then used to perform real-time water transfer factor measurements on both cathode and anode side of a PEMFC. The anode side measurements were found to be more reproducible than the cathode side measurements, by almost one order of magnitude. The water transfer factor profile along the flow channel direction was determined under several operating conditions for a 300 cm^2 co-current PEMFC by considering a series of six 50 cm^2 sub-cells. The measured water transfer factor profile was found to be in good agreement with the prediction from a recent model proposed by Berg et al. (12) under moderately high pressure (200 kPa) and current densities (above 0.3 A/cm^2). At lower current densities, the measured water transfer factors were found to be much lower than the model predictions. Similar results were found by measuring the water transfer while performing a polarization curve. These observation and experimental results will serve as basis for tailoring the model for current and new MEA designs.

ACKNOWLEDGEMENTS

The authors would like to express their gratitude to NSERC and Ballard Power Systems for a CRD grant (CRDPJ 3011929) supporting this work.

NOMENCLATURE

Symbol	Definition	Subscript	Definition
A	MEA surface area (cm^2)	a	Anode
F	Faraday constant	c	Cathode
I	Load (A)	$a \rightarrow c$	Anode to cathode transfer
j	Current density profile (A/cm^2)	in	PEMFC inlet
n	Molar flow rate (mol/s)	out	PEMFC outlet
Q	Flux across membrane ($\text{mol}/\text{cm}^2\text{s}$)	rx	Produced by reaction
x	Molar fraction	pre	Pre-injection, measurement concept 2
Greek letters		ref	Reference injection, measurement concept 3
α	Water transfer factor (local)	MFM_i	Mass flow meter (Figure 1)
$\bar{\alpha}$	Average water transfer factor	H_2O	Water
ν	Stoichiometric coefficients ($\nu_{H_2O} = 2, \nu_{H_2} = -2, \nu_{e^-} = 4$)	H_2	Hydrogen
		e^-	Electron

REFERENCES

1. G.J.M. Janssen and M.L.J. Overelde, "Water Transport in the Proton-Exchange-Membrane Fuel Cell: Measurements of the Effective Drag Coefficient," Journal of Power Sources, Vol. 101, No. 1, 2001, 117-125.
2. H.H. Voss, D.P. Wilkinson, P.G. Pickup, M.C. Johnson and V. Basura, "Anode Water Removal: A Water Management and Diagnostic Technique for Solid Polymer Fuel Cells," Electrochimica Acta, Vol. 40, No. 3, 1995, 321-328.
3. M.M. Mench, Q.L. Dong and C.Y. Wang, "In Situ Water Distribution Measurements in a Polymer Electrolyte Fuel Cell," Journal of Power Sources, Vol. 124, No. 1, 2003, 90-98.
4. T.E. Springer, T.A. Zawodzinski and S. Gottesfeld, "Polymer Electrolyte Fuel Cell Model," Journal of the Electrochemical Society, Vol. 138, No. 8, 1991, 2334-2342.
5. A.Z. Weber and J. Newman, "Modeling Transport in Polymer-Electrolyte Fuel Cells," Chemical Reviews, Vol. 104, No. 10, 4679-4726.
6. C.Y. Wang, "Fundamental Models for Fuel Cell Engineering," Chemical Reviews, Vol. 104, No. 10, 4727-4766.

7. T.A. Zawodzinski, T.E. Springer, F. Uribe and S. Gottesfeld, "Characterization of Polymer Electrolytes for Fuel Cell Applications," Solid State Ionics, Vol. 60, No. 1-3, 1993, 199-211.
8. T.A. Zawodzinski, C. Derouin, S. Radzinski, R.J. Sherman, V.T. Smith, T.E. Springer and S. Gottesfeld, "Water Uptake by and Transport through Nafion 117 Membranes," Journal of the Electrochemical Society, Vol. 140, No. 4, 1993, 1041-1047.
9. T. Okada, G. Xie, O. Gorseth, S. Kjelstrup, N. Nakamura and T. Arimura, Tomoaki, "Ion and Water Transport Characteristics of Nafion Membranes as Electrolytes," Electrochimica Acta, Vol. 43, No. 24, 1998, 3741-3747.
10. T.F. Fuller and J. Newman, "Experimental Determination of the Transport Number of Water in Nafion 117 Membrane," Journal of the Electrochemical Society, Vol. 139, No. 5, 1992, 1332-1337.
11. T.A. Zawodzinski, J. Davey, J. Valerio and S. Gottesfeld, Water Content Dependence of Electro-Osmotic Drag in Proton-Conducting Polymer Electrolytes, Electrochimica Acta, Vol. 40, No. 3, 1995, 297-302.
12. P. Berg, K. Promislow, J. St-Pierre, J. Stumper and B. Wetton, "Water Management in PEM Fuel Cells," Journal of the Electrochemical Society, Vol. 151, No. 3, 2004, A341-A353.
13. I.-M. Hsing and P. Futerko, "Two-Dimensional Simulation of Water Transport in Polymer Electrolyte Fuel Cells," Chemical Engineering Science, Vol. 55, No. 19, 2000, 4209-4218.
14. G. Karimi and X. Li, "Electroosmotic Flow through Polymer Electrolyte Membranes in PEM Fuel Cells," Journal of Power Sources, Vol. 140, No. 1, 2005, 1-11.
15. T.A. Zawodzinski, M. Neeman, L.O. Sillerud and S. Gottesfeld, "Determination of Water Diffusion Coefficients in Perfluorosulfonate Ionomeric Membranes," Journal of Physical Chemistry, Vol. 95, No. 15, 1991, 6040-6044.
16. V.T. Nguyen and N. Vanderborgh, Nicholas, "Rate of Isothermal Hydration of Polyperfluorosulfonic Acid Membranes," Journal of Membrane Science, Vol. 143, No. 1-2, 1998, 235-248. (Erratum see Vol. 192, No. 1-2, 2001, 249).
17. T. Okada, S. Moller-Holst, O. Gorseth and S. Kjelstrup, "Transport and Equilibrium Properties of Nafion Membranes with H⁺ and Na⁺ Ions," Journal of Electroanalytical Chemistry, Vol. 442, No. 1-2, 1998, 137-145.
18. J. Stumper, S.A. Campbell, D.P. Wilkinson, M.C. Johnson and M. Davis, "In-Situ Methods for the Determination of Current Distributions in PEM Fuel Cells," Electrochimica Acta, Vol. 43, No. 24, 1998, 3773-3783.